

A sceptical analysis of Quantized Inertia

Michele Renda,¹[★]

¹ *Department of Elementary Particle Physics, IFIN-HH, Reactorului 30, P.O.B. MG-6, 077125, Măgurele, Romania*

Accepted XXX. Received YYY; in original form ZZZ

ABSTRACT

We perform an analysis of the derivation of Quantized Inertia (QI) theory, formerly known with the acronym MiHsC, as presented by McCulloch (2007, 2013). Two major flaws were found in the original derivation. We derive a discrete black-body radiation spectrum, deriving a different formulation for $F(a)$ than the one presented in the original theory. We present a numerical result of the new solution which is compared against the original prediction.

Key words: dark matter – galaxies: kinematics and dynamics – cosmology: theory

1 INTRODUCTION

The discrepancy between observed galaxies rotation curves and the prediction using the known laws of orbital kinematics was initially observed by Rubin et al. (1980), and it is now an accepted phenomenon.

Several theories were developed to justify such discrepancies, such as the existence of a dark matter halo (Rubin 1983), or the existence of a Modified Newtonian Dynamics, MoND (Milgrom 1983) at galactic scales.

As today, no direct evidence of dark matter was detected, though many experiments such as XENON100 (Aprile et al. 2012) and SuperCDMS (SuperCDMS Collaboration et al. 2014) are looking for signal candidates. Some models support the idea that dark matter particles could be created at LHC and efforts in this direction are in progress (Abercrombie et al. 2015; Mitsou 2015; Liu et al. 2019).

MoND models remove the necessity for dark matter candidates introducing a modified law of motion for low accelerations:

$$F = \begin{cases} ma & \text{when } a \gg a_0 \\ m \frac{a^2}{a_0} & \text{when } a \ll a_0 \end{cases} \quad [N] \quad (1)$$

This approach has been criticized due to the requirement of an arbitrary parameter a_0 and because it does not predict the dynamics of galaxy clusters (Aguirre et al. 2001; Sanders 2003). A new theory, by McCulloch, proposes a solution to the discrepancies observed in the galaxies' rotation curves. This theory, named Modification of inertia resulting from a Hubble-scale Casimir effect (MiHsC) or Quantized Inertia (QI), may give a model for the galaxies' rotation curves (McCulloch 2012) and explain some other phe-

nomena like the Pioneer anomaly (McCulloch 2007), the flyby anomalies (McCulloch (2008), the Em-drive (McCulloch 2015), opening the way for propellant-less spacecraft propulsion (McCulloch 2018). In addition, this theory provides also an intuitive explanation for objects' inertia (McCulloch 2013).

The main strong points of this theory, as shown by eq. (7), are the absence of arbitrary tunable parameters (being based on universal constants like the Hubble constant and the speed of light), its simple formulation and the wide range of phenomena it seems to explain. Its main weak point is the fact it assumes the existence of the Unruh radiation (Unruh 1976), which is still not experimentally measured in nature, although some recent simulations seems to confirm its existence (Hu et al. 2019).

Quantized Inertia has collected some criticisms by mainstream press (Koberlein 2017), but, as today, no critical analysis was published in a peer-reviewed journal on this subject.

In the next sections we will present our analysis of Quantized Inertia: in section 2 we will perform a brief recapitulation of the theory as presented by McCulloch (2007, 2013), in sections 3 and 4 we will present two major flaws we found in its derivation and we propose some corrections and finally, in section 5, we will present our considerations about the validity of the whole theory.

2 RECAPITULATION ON QUANTIZED INERTIA

Quantized Inertia states two important affirmation:

- (i) There exists a minimum acceleration any object can ever have: $a_0 = 2c^2/\Theta = 2 \times 10^{-10} \text{ m s}^{-2}$ (see McCulloch 2017, sect. 2). Below such a value, the object's inertia becomes zero

[★] E-mail: michele.renda@cern.ch

causing the object's acceleration to increase to the minimum value.

(ii) Inertia is caused by the Unruh radiation imbalance between the cosmic and the Rindler horizon (McCulloch 2013, fig.1).

The rationale behind the first point is this: according to the Unruh radiation law (Unruh 1976), every accelerating object will feel a background temperature:

$$T = \frac{\hbar a}{2\pi c k} \quad [\text{K}] \quad (2)$$

where \hbar is the reduced Planck constant, c the speed of light in vacuum, k the Boltzmann constant and a the object's acceleration. It is important to notice that this temperature is very tiny: for an object acceleration of 1 m s^{-2} , the temperature will be $T \approx 4 \times 10^{-21} \text{ K}$, making very difficult any experimental detection.

Planck's law states such background will emit black-body radiation with spectrum:

$$b_\lambda(\lambda, T) = \frac{2hc^2}{\lambda^5} \frac{1}{e^{hc/\lambda kT} - 1} \quad [\text{W m}^{-1} \text{ sr}^{-1} \text{ m}^{-2}] \quad (3)$$

with a peak wavelength:

$$\lambda_{\text{peak}} = \frac{hc}{a_5 kT} \quad [\text{m}] \quad (4)$$

where $a_5 \approx 4.96511423174$ is the solution of the transcendental equation $5(1 - e^{-x}) = x$ and h is Planck's constant. We would like to remark that the Planck's law describes an *unconstrained* system at equilibrium. This is the case in a classic black-body radiation experiment where the radiation wavelength is much smaller than the cavity size, leading to a continuous spectrum.

However, for very low temperatures, the associated radiation wavelength may become bigger than the cosmic horizon, defined as the sphere with radius equal to the Hubble distance. We introduce so the Hubble diameter defined as:

$$\Theta = \frac{2c}{H_0} \approx 2.607 \times 10^{26} \text{ m} \quad (5)$$

where H_0 is the Hubble constant¹ and c is the speed of light in vacuum. In this case we can not consider the spectra continuous any more, because, by principle, only the wavelengths fitting twice the Hubble diameter can ever exist:

$$\lambda_n = \frac{2\Theta}{n} \quad \text{where } n = 1, 2, 3, \dots, \infty \quad [\text{m}] \quad (6)$$

The minimum acceleration arises from two phenomena: for lower accelerations, the object experiences lower Unruh background radiation due to a) the shift of the spectra behind the Hubble diameter and b) a more sparse sampling of the black body radiation spectra, as shown in fig. 1.

The consideration expressed above were used to define a Hubble Scale Casimir-like effect: using a not better specified *direct calculation*, McCulloch (2007, sect. 2.2) affirms there is a linear relation between the continuous and the discrete sampling of the Unruh radiation spectra. The ratio between the two sampling, denoted with $F(a)$, is considered to be

¹ In this paper we assume $H_0 = 2.3 \pm 0.9 \times 10^{-18} \text{ s}^{-1}$, as used by McCulloch (2007, sect. 2.1), for easier results comparison with the original papers.

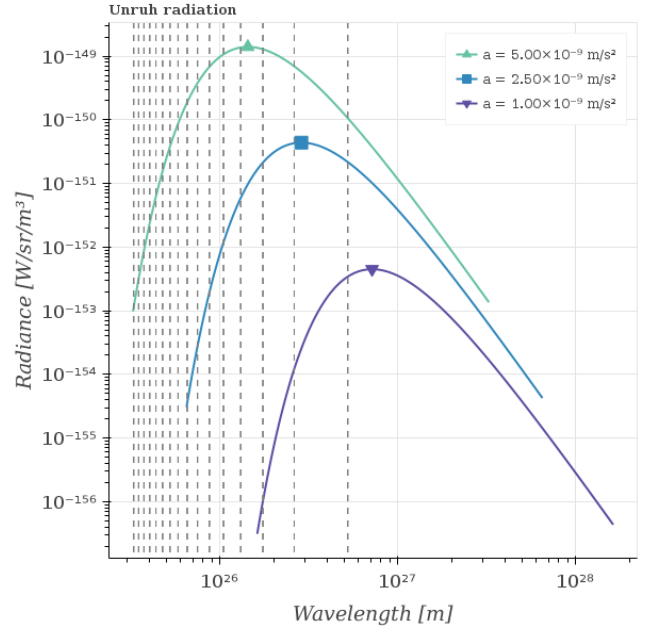


Figure 1. Plot of the Unruh radiation spectra for different object accelerations. The marks represent the λ_{peak} for the given acceleration. The last dashed line on the right represents the biggest wavelength fitting inside twice the Hubble diameter.

a linear function. Assuming that for $\lambda_{\text{peak}} \rightarrow 0$ we have the classical case ($F = 1$), and for $\lambda_{\text{peak}} \rightarrow 4\Theta$ no Unruh radiation is sampled ($F = 0$), this relation was proposed by McCulloch (2007):

$$m_I = F(a) m_i = \left(1 - \frac{\beta\pi^2 c^2}{a\Theta}\right) m_i \quad [\text{kg}] \quad (7)$$

where $\beta = 1/a_5 \approx 0.2$, a is the acceleration modulus, m_i is the classic inertial mass and m_I the modified inertial mass.

3 CORRECTION 1

We focus our attention on the derivation of eq. (7), based on the linear relation:

$$m_I = F(a) m_i = \frac{B_s(a)}{B(a)} m_i \quad [\text{kg}] \quad (8)$$

where B_s is the sampled (discrete) black body radiance and B is the classical one. The value of B can be found integrating eq. (3):

$$B(T) = \int_0^\infty b_\lambda(\lambda, T) d\lambda = \frac{2\pi^4 k^4}{15h^3 c^2} T^4 \quad [\text{W m}^{-2} \text{ sr}^{-1}] \quad (9)$$

while the determination of B_s is more complex and will be discussed in section 3.2.

3.1 Derivation of Planck's law for unconstrained cavities

If we have a cubic cavity with side L , we can have an infinite number of independent radiation modes. Each mode can be

defined by three non-negative integers, l, m, n , such that the wave fits entirely in twice the cavity side:

$$\lambda_x = \frac{2L}{l} \quad \lambda_y = \frac{2L}{m} \quad \lambda_z = \frac{2L}{n} \quad [\text{m}] \quad (10)$$

Using this notation, it is possible to define a new quantity named wave-vector defined as:

$$k_x = \frac{2\pi}{\lambda_x} = \frac{\pi l}{L} \quad k_y = \frac{2\pi}{\lambda_y} = \frac{\pi m}{L} \quad k_z = \frac{2\pi}{\lambda_z} = \frac{\pi n}{L} \quad [\text{m}^{-1}] \quad (11)$$

so any wave can be expressed as:

$$A(\mathbf{r}, t) = A_0 \sin(\mathbf{k} \cdot \mathbf{r} - \omega t) \quad (12)$$

Using this formalism, we can express each wave in a cavity using three non-negative integers, l, m, n : smaller integers represent longer wavelengths, while higher values represent shorter ones. We can represent these points in a graph, as shown in fig. 2.

Every point represents a wave-mode in the cavity: the points with the same modulo will have the same energy, or, more concisely, if we define $p^2 = l^2 + m^2 + n^2$, for the same value of p , we have the same energy. The relation between λ and p now becomes:

$$\lambda = \frac{2L}{p} \quad [\text{m}] \quad (13)$$

If we want to calculate the energy density, we have to sum the number of wave-modes with the same energy multiplied by their average energy and divide by volume:

$$U(T) = \sum_p u(p, T) = \sum_p \frac{2 N(p) \bar{E}(p, T)}{L^3} \quad [\text{J m}^{-3}] \quad (14)$$

where $N(p)$ is the number of independent modes with wave-mode p , $\bar{E}(p)$ is the average energy of that mode and the factor 2 reflects the fact that each wave can have two independent polarizations. $\bar{E}(p)$ can be found using the Boltzmann distribution:

$$\bar{E}(p, T) = E_p \frac{e^{-\frac{E_p}{kT}}}{\sum_{p^2=1}^{\infty} e^{-\frac{E_p}{kT}}} = \frac{hc}{\lambda_p} \frac{1}{e^{hc/\lambda_p kT} - 1} \quad [\text{J}] \quad (15)$$

where $\lambda_p = 2L/p$ and $E_p = hc/\lambda_p$.

For the determination of $N(p)$, we need to estimate the number of wave-modes for a given energy: for an unconstrained system, when $\lambda_{\text{peak}} \ll L$, we can suppose the wave-modes are so dense we can estimate them as the volume of a shell of a sphere with radius p and thickness dp (as shown in fig. 2a):

$$\bar{N}(p) dp = \frac{1}{8} 4\pi p^2 dp \quad (16)$$

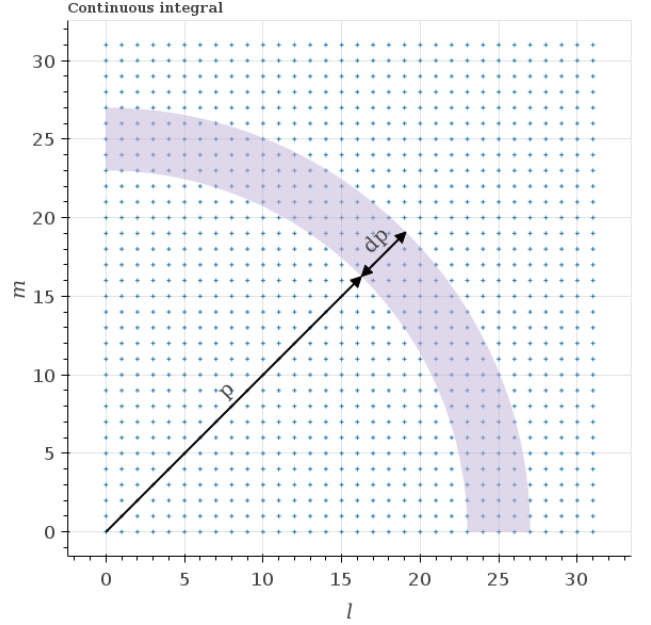
where the factor 1/8 reflects the fact we are only counting one octant ($l, m, n > 0$). We can now transform eq. (14) into a *continuous* sum, by frequency ($\nu = cp/2L$) or by wavelength ($\lambda = 2L/p$):

$$U(T) = \int u(\nu, T) d\nu = \int u(\lambda, T) d\lambda \quad [\text{J m}^{-3}] \quad (17)$$

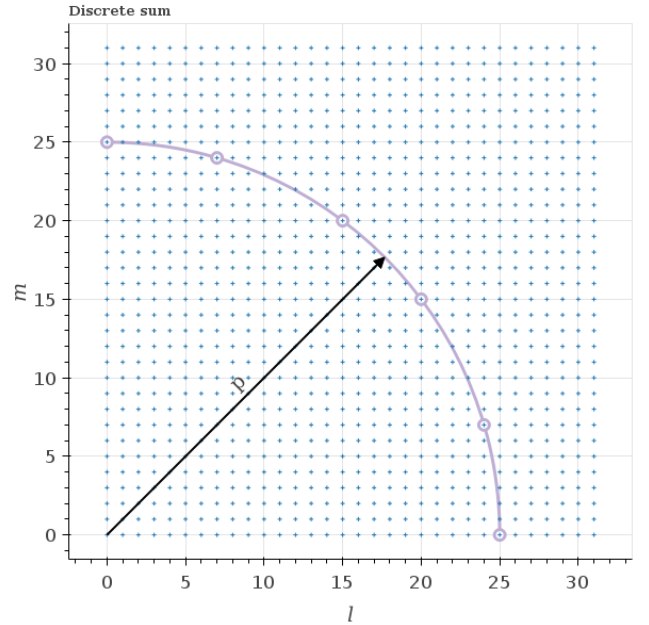
where

$$u(\nu, T) = \frac{8\pi h\nu^2}{c^3} \frac{1}{e^{h\nu/kT} - 1} \quad [\text{J Hz}^{-1} \text{m}^{-3}] \quad (18)$$

$$u(\lambda, T) = \frac{8\pi hc}{\lambda^5} \frac{1}{e^{hc/\lambda kT} - 1} \quad [\text{J m}^{-1} \text{m}^{-3}] \quad (19)$$



(a) Continuous integral



(b) Discrete sum

Figure 2. Plane section of the l, m, n volume: each cross represents a wave-mode. Points near to the origin will have longer wavelengths while points with the same modulus will share the same wavelength and energy.

Equations (18) and (19) are often presented in the form of power radiance, which can be found multiplying them by $c/4\pi$:

$$b(\nu, T) = \frac{2h\nu^3}{c^2} \frac{1}{e^{h\nu/kT} - 1} \quad [\text{W Hz}^{-1} \text{sr}^{-1} \text{m}^{-2}] \quad (20)$$

$$b(\lambda, T) = \frac{2hc^2}{\lambda^5} \frac{1}{e^{hc/\lambda kT} - 1} \quad [\text{W m}^{-1} \text{sr}^{-1} \text{m}^{-2}] \quad (21)$$

3.2 Derivation of Planck's law for constrained cavities

In section 3.1 we discussed the derivation of Planck's law because now we will use the same principle to derive a similar equation for constrained cavities, where the wavelength sizes are comparable to the cavity dimensions. This time we can not transform eq. (14) in a continuous sum, but we have to handle it as an infinite *discrete* sum.

The value of $E(p, T)$ can be found using the Boltzmann distribution:

$$\bar{E}(p, T) = \bar{E}_{\lambda_p=2L/p}(\lambda_p, T) = \frac{hc}{\lambda_p} \frac{1}{e^{hc/\lambda_p kT} - 1} \quad [\text{J}] \quad (22)$$

while the value N_p are the number of modes where $l^2 + m^2 + n^2 = p^2$, as shown in fig. 2b. Unfortunately, this value can not be calculated analytically but, if we define $n = p^2$ we can find the value of $N(p)$ in the sequence A002102 (Sloane & Plouffe 1995). Using this definition, eqs. (19) and (21) become, respectively:

$$u_s(p, T) = \frac{2N(p)}{L^3} \frac{hc}{\lambda_p} \frac{1}{e^{hc/\lambda_p kT} - 1} \quad [\text{J m}^{-3}] \quad (23)$$

$$b_s(p, T) = \frac{2N(p)}{L^3} \frac{hc^2}{4\pi\lambda_p} \frac{1}{e^{hc/\lambda_p kT} - 1} \quad [\text{W sr}^{-1} \text{ m}^{-2}] \quad (24)$$

where $\lambda_p = 2L/p$. Finally, we can find the sum for all the modes as:

$$U_s = \sum_{p^2=1}^{\infty} u_s(p, T) \quad [\text{J m}^{-3}] \quad (25)$$

$$B_s = \sum_{p^2=1}^{\infty} b_s(p, T) \quad [\text{W sr}^{-1} \text{ m}^{-2}] \quad (26)$$

3.3 Ratio between B_s and B

Using the results from the previous section and eqs. (5), (8) and (13), now it is possible to find a new expression for the function $F(T)$:

$$F(T) = \frac{15H_0^4 h^4}{128\pi^5 k^4 T^4} \sum_{p^2=1}^{\infty} N(p) \frac{p}{e^{hp/4H_0 kT} - 1} \quad (27)$$

which can be expressed, using eq. (2), as a function of the object's acceleration:

$$F(a) = \frac{30\pi^3 H_0^4 c^4}{a^4} \sum_{p^2=1}^{\infty} N(p) \frac{p}{e^{p\pi^2 c H_0/a} - 1} \quad (28)$$

The term $N(p)$ make very difficult any analytical solution of eq. (28), but it is possible to solve numerically, as shown in fig. 3. We can observe it is different from eq. (7): while we can observe that for $a > 1 \times 10^{-8} \text{ m s}^{-2}$, $F = 1$ (classical case), and for $a < a_0$, $F = 0$, as predicted by McCulloch (2007), but we also have a critical point at $a_p \approx 1.20 \times 10^{-9} \text{ m s}^{-2}$ where we have a maximum value for $F \approx 2.17$.

This point would represent a stable point because, if we apply a small force to an object around this critical value, the shape of $F(a)$ will stabilize the object's acceleration. At the knowledge of the authors, no such behaviour was ever measured or predicted theoretically by other models.

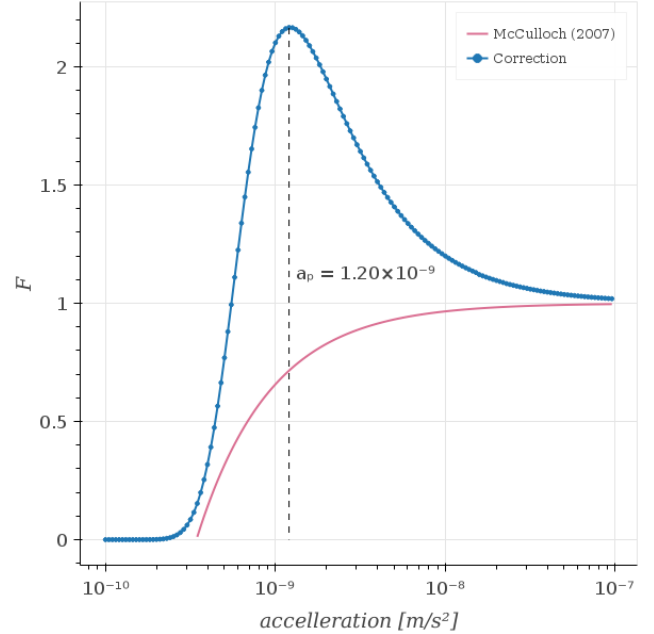


Figure 3. Plot of the $F(a) = B_s(a)/B(a)$ function for low accelerations. We can observe that $F(a \rightarrow \infty) = 1$ (classical case) and $F(a \rightarrow 0) = 0$ and a peak around $a_p \approx 1.20 \times 10^{-9} \text{ m s}^{-2}$. The marks represent the values in which the calculation was performed.

4 CORRECTION 2

In this section, we will discuss the radiation imbalance between the Cosmic and Rindler horizon. In McCulloch (2013), it is shown how applying eq. (7) to an object moving along the direction x , as shown in fig. 4, there will be an imbalance between the radiation pressure on the right, limited by the cosmic horizon, and the radiation pressure on the left, limited by the nearer Rindler horizon.

This radiation pressure imbalance will cause a force reacting against any acceleration similar in behaviour to the classical inertia. It is shown in McCulloch (2013) (and partially corrected by Giné & McCulloch (2016)), it is possible to express the force \mathbf{F} as:

$$\mathbf{F} = -\frac{\pi^2 h A}{48cV} \mathbf{a} \quad [\text{N}] \quad (29)$$

where A is the object's radiation cross-section, smaller than the physical cross-section, V is the object's volume and a the modulus of the object's acceleration.

It is also shown that, if we assume the particle a cube with size equal to the Planck's length, $l_P = 1.616 \times 10^{-35} \text{ m}$, the model predicts an inertial mass of $2.799 \times 10^{-8} \text{ kg}$, which is 29% greater than the Planck's mass, $m_P = 2.176 \times 10^{-8} \text{ kg}$ (Giné & McCulloch 2016).

Our main concern is how the energy density substitution was performed in both McCulloch (2013, eq. 9-10) and Giné & McCulloch (2016, eq. 7-8):

$$u = \frac{E}{V} = \frac{hc}{\lambda V} \quad [\text{J m}^{-3}] \quad (30)$$

In this substitution, the authors imply that only the peak wavelength of the Unruh spectrum contributes to the energy densities. In reality, this is deeply incorrect because

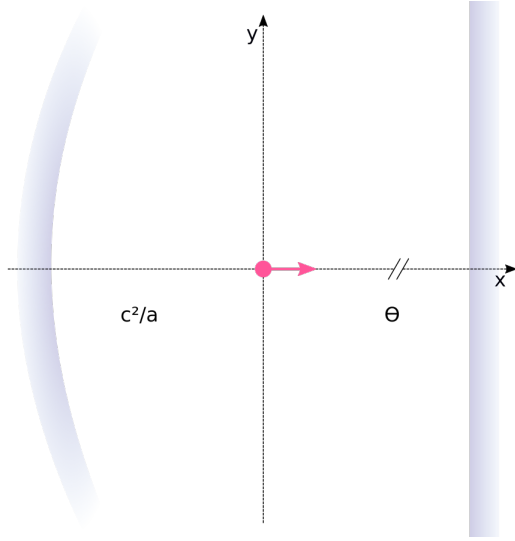


Figure 4. Schematic representation of the Cosmic and Rindler horizon as presented by McCulloch (2013). If the object is accelerating to the right a Rindler horizon is formed on the left, disallowing some Unruh waves on that side and, consequentially, a lower radiation pressure. The radiation pressure imbalance will produce a force against the direction of acceleration.

for classical accelerations (i.e. $a > 1 \times 10^{-8} \text{ m s}^{-2}$), the peak wavelength contributes only a tiny part of the overall energy density. We can define a new quantity G , expressing the contribution of the peak wavelength to the radiation energy density as:

$$G(a) = \frac{u_s(p', a)}{U_s(a)} = \frac{N(p') \frac{p'}{e^{p'\pi^2 c H_0/a} - 1}}{\sum_{p^2=1}^{\infty} N(p) \frac{p}{e^{p\pi^2 c H_0/a} - 1}} \quad (31)$$

where p' is the wave-mode nearest to the peak wavelength, which can be calculated as:

$$p' = \sqrt{\text{round}\left(\frac{a_5 a}{\pi^2 c H_0}\right)^2} \quad (32)$$

In figure fig. 5, we can see the plot of $G(a)$ over a range of different accelerations, and we can notice that for classical accelerations, eq. (30) it is wrong in principle.

5 CONCLUSIONS

In this paper we analysed two main articles (McCulloch 2007, 2013) describing Quantized Inertia. We found two major flaws on the derivation presented, and we propose some corrections to address the found issues. Such flaws, if they do not invalidate, at least will require a major rethinking of the whole theory. In our article, we did not address the ability of Quantized Inertia to match the observational data.

We consider that speculative physics is fundamental for the constant progress of science: Quantized Inertia was often criticized because it does go against well-established principles such as the equivalence principle. We consider this should not be the criterion used to establish the validity of a theory: history teaches us that many scientific breakthroughs, encountered, in the beginning, strong resistance

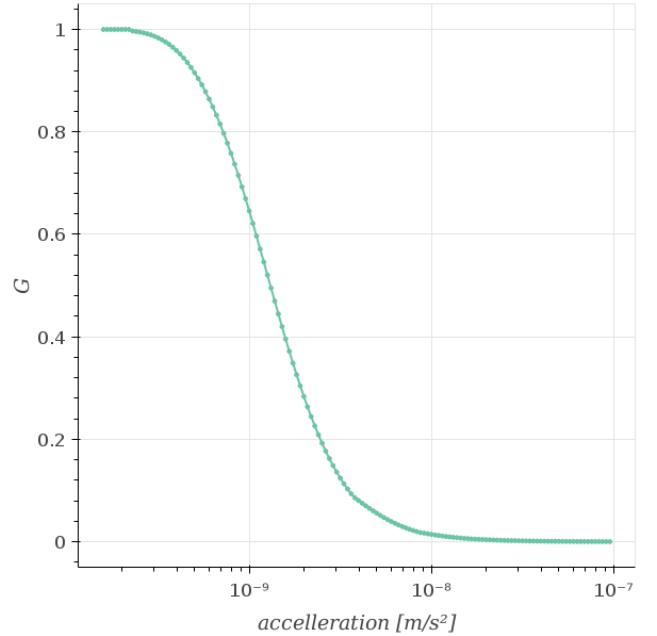


Figure 5. Plot of $G(a)$: it shows the contribution of the highest u_s over the entire spectrum. For lower accelerations this value is near to one because only a few modes are allowed but for higher accelerations its contribution tends to zero.

from the scientific community because they were against existing principles. For this reason, it is of fundamental importance that any new iteration of quantized inertia should have a stronger mathematical derivation and, eventually, a strategy for a practical experimental verification.

ACKNOWLEDGEMENTS

This work was supported by the research project PN19060104. We would like to thank our ATLAS group colleagues for the supportive working environment and in particular Prof. Călin Alexa for his guidance and support during the writing of this article. We would like also to thanks the [Bokeh Development Team \(2014\)](#) for the excellent tool used to create the plots of this paper and the reviewer of this article for his meaningful feedbacks and the intellectual integrity shown during the review process.

REFERENCES

- Abercrombie D., et al., 2015, Technical Report FERMILAB-PUB-15-282-CD, Dark Matter Benchmark Models for Early LHC Run-2 Searches: Report of the ATLAS/CMS Dark Matter Forum. CERN ([arXiv:1507.00966](#))
- Aguirre A., Schaye J., Quataert E., 2001, *ApJ*, 561, 550
- Aprile E., et al., 2012, *Astropart. Phys.*, 35, 573
- Bokeh Development Team 2014, Bokeh: Python library for interactive visualization. <http://www.bokeh.pydata.org>
- Giné J., McCulloch M. E., 2016, *Mod. Phys. Lett. A*, 31, 1650107
- Hu J., Feng L., Zhang Z., Chin C., 2019, *Nat. Phys.*, pp 1–9
- Koberlein B., 2017, Quantized Inertia, Dark Matter, The EM-Drive And How To Do Science Wrong, <https://tinyurl.com/forbes-quantized-inertia>

- Liu J., Liu Z., Wang L.-T., 2019, *Phys. Rev. Lett.*, 122, 131801
McCulloch M. E., 2007, *MNRAS*, 376, 338
McCulloch M. E., 2008, *MNRAS Lett.*, 389, L57
McCulloch M. E., 2012, *Ap&SS*, 342, 575
McCulloch M. E., 2013, *EPL*, 101, 59001
McCulloch M. E., 2015, *EPL*, 111, 60005
McCulloch M. E., 2017, *Astrophys. Space Sci.*, 362, 57
McCulloch M. E., 2018, *J. Space Expl.*, 7, 1
Milgrom M., 1983, *ApJ*, 270, 365
Mitsou V. A., 2015, *J. Phys.: Conf. Ser.*, 651, 012023
Rubin V. C., 1983, *Science*, 220, 1339
Rubin V. C., Ford Jr. W. K., Thonnard N., 1980, *ApJ*, 238, 471
Sanders R. H., 2003, *MNRAS*, 342, 901
Sloane N., Plouffe S., 1995, *The Encyclopedia of Integer Sequences*, 1st edition edn. Academic Press
SuperCDMS Collaboration et al., 2014, *Phys. Rev. Lett.*, 112, 241302
Unruh W. G., 1976, *Phys. Rev. D*, 14, 870

This paper has been typeset from a $\text{\TeX}/\text{\LaTeX}$ file prepared by the author.